



An efficient multiple-mode molecular logic system for pH, solvent polarity, and Hg²⁺ ions

Dong Zhang, Jianhua Su, Xiang Ma, He Tian*

Key Laboratory for Advanced Materials and Institute of Fine Chemicals, East China University of Science and Technology, Shanghai 200237, PR China

ARTICLE INFO

Article history:

Received 29 February 2008
Received in revised form 25 April 2008
Accepted 9 May 2008
Available online 14 May 2008

Keywords:

Molecular logic gate
Hg sensor
pH switch

ABSTRACT

A novel fluorophore 1,3-bis(1,1,3-trimethyl-1*H*-benzo[*e*]indol-2(3*H*)-ylidene)propan-2-one (**L**) was synthesized and fully characterized by ¹H NMR, ¹³C NMR, HRMS, and X-ray single-crystal structural analysis. Compound **L** is a pH-controlled molecular switch due to its protonation. The fluorescence change in protic polar solvents means that this compound also could be used as a protic solvent polarity sensor. Among the considered metal ions, the fluorescence of compound **L** could be quenched completely by Hg²⁺ ions with a high selectivity. Based on these fluorescence characters, this fluorescent dye **L** has promising applications as a multiple-mode molecular logic system.

© 2008 Elsevier Ltd. All rights reserved.

1. Introduction

Developing a wide variety of supramolecular systems performing as elementary electronic devices, such as switches, sensors, logic gates, and molecular-level machines, is an intense research area and of tremendous significance to the development of miniaturized device components.¹ Potential applications of these components in optical and electronic molecular-scale computational devices have attracted considerable effort to this research area.²

A significant amount of work has been devoted to obtain specific molecule that is able to change one or several macroscopic properties in response external inputs.³ The design of fluorescent signaling molecules has attracted a great deal of attention.⁴ Many supramolecular systems, the emission properties of which can be modulated by external inputs, such as temperature, pH, redox potential, solvent polarity, and metal ions, have been reported.^{5–9} There are few molecular systems behaving as ‘multiply configurable’ fluorescent indicators.¹⁰

Merocyanine dyes are heterocyclic chromophores that are extensively used in a number of areas (i.e., as photographic sensitizers, for nonlinear optics, and in chemotherapy).¹¹ Recently, they have also been employed as sensors of protein conformation and protein interactions in live cell imaging.¹² Here, we design a merocyanine dye, **L** (Scheme 1), which has a carbonyl bearing two benzo[*e*]indoline fragments at both ends. At both sides, **L** has

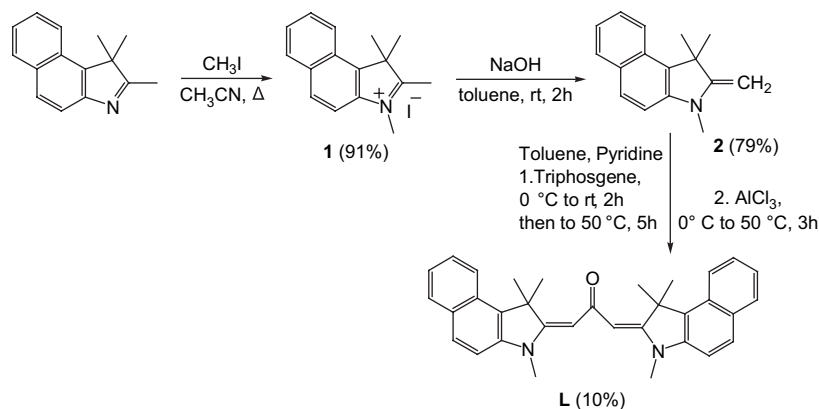
nitrogen atoms (trialkylamine moiety), which could be protonated. In fact, basic donor amino groups can also act as fluorescence quenchers.¹³ On account of the nitrogen atoms with lone electron pairs, which can form coordinate bonds, **L** is propitious to recognize special metal ion with high selectivity due to its structure. Based on these results, a pH switch was achieved. Meanwhile, a highly fluorescent material displaying novel solvent polarity-tunable blue-green fluorescence emission was presented, which was clearly different from the behaviors of solvent polarity sensors previously reported. Otherwise, this molecule has a selective detection of Hg²⁺ ions.

As a class of molecular devices, fluorescent logic gates play a pivotal role in molecular computation because they are detectable as a single molecule and can simultaneously treat multiple inputs.^{14,15} Within the past decade, many fluorescent logic gates showing NOT, AND, OR, XOR, NOR, NAND, and INHIBIT operations, and combinational logic circuits incorporating single logic gates have been reported.¹⁶ In the same way, the molecule we reported here could demonstrate three different logic functions (NAND, NOR, and INHIBIT) operated by solvent polarity, proton (H⁺), and Hg²⁺ as inputs.

2. Results and discussion

The synthetic route to the merocyanine receptor (**L**) is illustrated in Scheme 1. 1,1,2,3-Tetramethyl-1*H*-benzo[*e*]indolinium iodide (**1**) and 2-methylene-1,1,3-trimethyl-1*H*-benzo[*e*]indoline (**2**) were prepared according to the literature method.¹⁷ Treatment of **2** with an appropriate amount of triphosgene and AlCl₃ afforded the symmetrical structural **L**. Compounds **1**, **2**, and **L** have been

* Corresponding author. Tel.: +86 21 64252756; fax: +86 21 64252288.
E-mail address: tianhe@ecust.edu.cn (H. Tian).



Scheme 1. Synthesis of merocyanine receptor **L**.

characterized by ^1H NMR spectroscopy, ^{13}C NMR spectroscopy, and HRMS (ESI) spectrometry. Compound **L** was also characterized crystallographically.

2.1. pH switch

Molecular systems behaving as a fluorescent indicator of the pH window have attracted much attention, because the proton (H^+) concentration is simply and easily controlled.¹⁸ Due to the very low solubility of **L** in water, its properties as a base have been examined in a THF/ H_2O mixed solvent. A 50% THF solution of **L** (1.0×10^{-5} M) was titrated with H^+ (HClO_4). After addition of H^+ , the yellow solution of **L** turned colorless (see the photograph in Fig. 1a). The color bleaching resulted from the progressive disappearance of the absorption band at 441 nm. Meanwhile, upon addition of H^+ , a new smaller absorption band with a peak at 393 nm forms and develops, as shown in Figure 2. The absorption makes a blue shift of 48 nm. There is no absorption from 500 to 700 nm, so this segment is not shown in Figure 2.

As shown in the photograph (Fig. 1b), the solution of **L** in 50% THF emits blue fluorescence, which can be considered as 'switched on'. Upon addition of H^+ , the blue fluorescence was quenched gradually. It was quenched completely at $\text{pH}=2$, which is considered as 'switched off' as shown in Figure 3. Since compound **L** is not 'ideal' polymethine, the mirror-image relationship of absorption and fluorescence is often abrogated.

In this pH sensing system, with a decrease in pH of the solution, the color was bleached and the fluorescence quenched. This change occurs because of the protonation of the nitrogen atoms (two trialkylamine moieties). The nitrogen atoms change from electron-contributing groups to electron-withdrawing units. After the

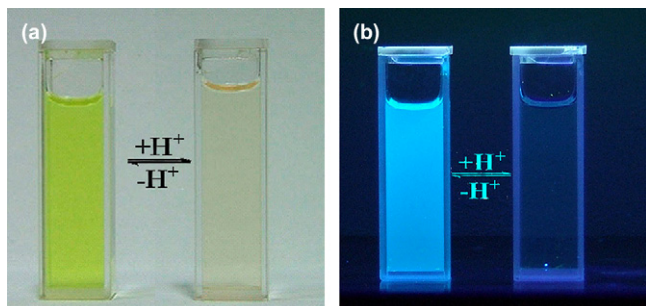


Figure 1. The color change (a) and fluorescence emission (b) responses of **L** (1.0×10^{-5} M in THF/ $\text{H}_2\text{O}=1:1$) on addition of H^+ . Left to right: in the absence ($\text{pH}=8$) and presence ($\text{pH}=2$) of H^+ in KCl (0.1 M) solution at 298 K.

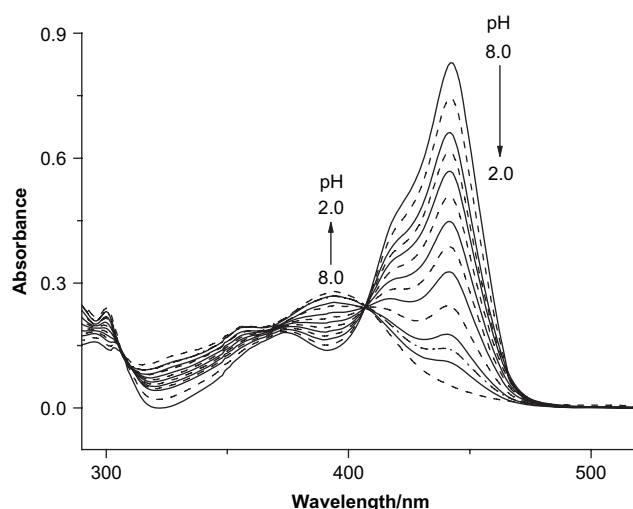


Figure 2. UV-vis spectra in the course of titration of the aqueous THF solution (1.0×10^{-5} M) of **L** with H^+ , at 298 K.

protonation, the whole conjugated system of the molecule has been separated. Thus, the merocyanine-like chromophore was broken up, which resulted in the blue shift of the absorption spectrum and the quenching of the fluorescence.

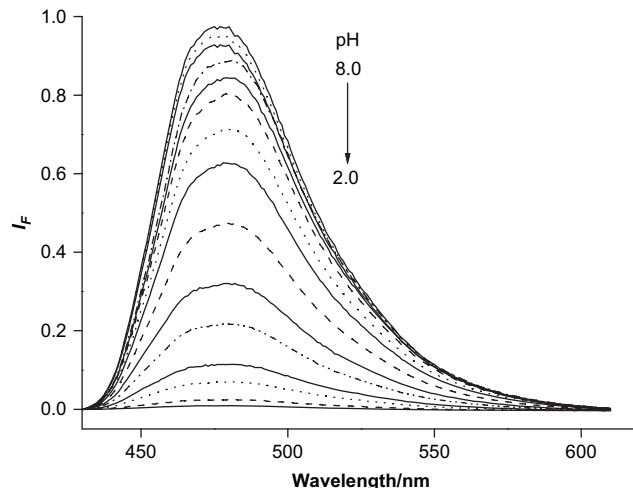


Figure 3. Change in fluorescence spectra ($\lambda_{\text{ex}}=410$ nm) of **L** (10 μM) with pH in aqueous KCl (0.1 M) solution with 50% THF at 298 K.

2.2. Polar fluorescence

There have been several experimental and theoretical studies on the solvatochromic behavior of merocyanine dyes.^{11a,19} As a merocyanine dye, the spectral character of compound **L** may be largely influenced in solvents of different polarities. We took the binary mixed solvents, THF with relative lower polarity and H₂O with higher polarity, to adjust the polarity of solvent. The emission spectra of **L** were recorded with different fractions of THF in distilled water (Fig. 4).

As the addition of a high-polarity solvent (H₂O) to a low-polarity one (THF), enhancement of the solvent polarity causes a significant quenching of the fluorescence of **L** coupled with the appearance of a new band centered at 520 nm. A dramatic fluorescence change from blue (95% THF) to green (5% THF) could be clearly seen (Fig. 5).

The dual emission character of this compound shows an obvious red shift. A well-defined isoemissive point at 508 nm can be clearly observed (Fig. 4). This could be interpreted in terms of two emissive species with a relationship, as one of the proofs for the formation of the exciplex with a polar solvent.²⁰ We have measured the fluorescence spectrum of **L** in different polar mixed solvents (Fig. 6).

Due to the low solubility of **L**, its fluorescence spectra were measured in different polar solvents containing 5% THF. Upon enhancement of the solvent polarity (THF → CH₃CH₂OH → CH₃OH → H₂O), the fluorescence of **L** makes a red shift and the intensity is weakened. This is probably due to the interaction between the

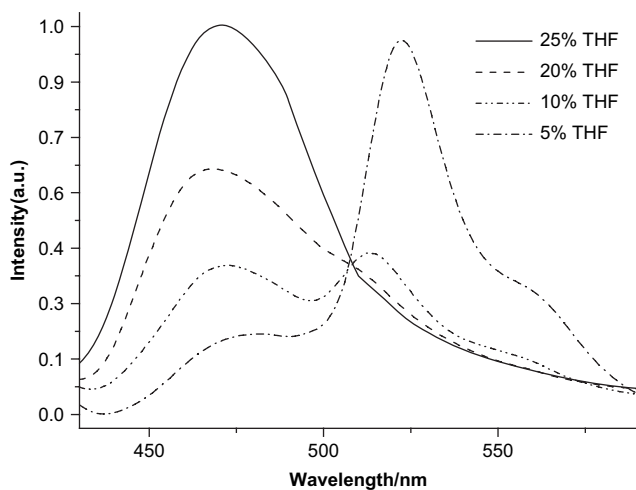


Figure 4. Emission spectra of **L** (1.0×10^{-5} M, at 298 K) in H₂O with different amount of THF excited at 410 nm.

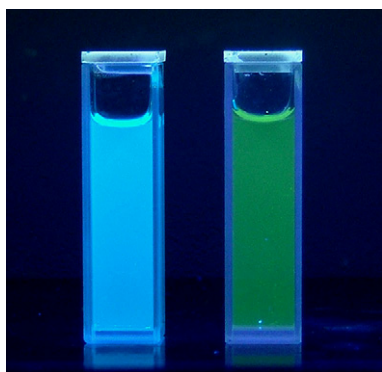


Figure 5. Photograph of **L** in 95% THF (left) and 5% THF (right), excited at 410 nm (1.0×10^{-5} M, at 298 K).

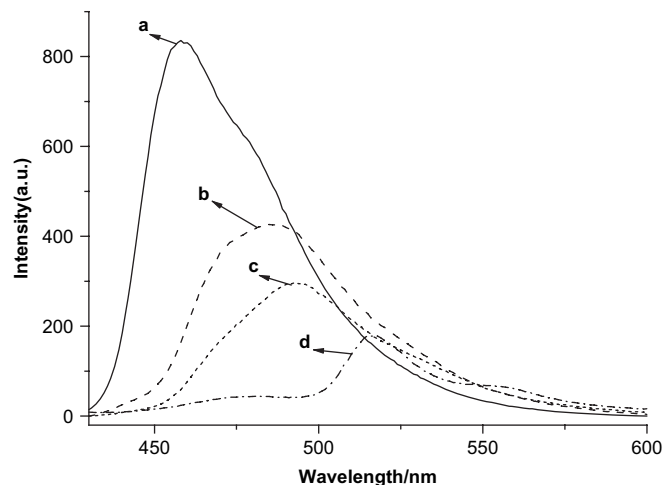


Figure 6. Emission spectra of **L** in mixed solvents with different polarities excited at 410 nm (1.0×10^{-5} M, at 298 K). From left to right: (a) pure THF; (b) 95% ethanol+5% THF; (c) 95% methanol+5% THF; (d) 95% H₂O+5% THF.

solvent and the merocyanine molecule. These indicated that **L** might be used as a solvent polarity sensor.

2.3. Metal ions

Sensing harmful species is critical to the environment. Elementary mercury and Hg²⁺ salts, which are dangerous for human health, should be detected effectively.²¹ Hg²⁺ is able to quench the fluorescence of **L** when forming the corresponding complex giving rise to the appearance of CHEQ (chelation enhanced quenching) effect. The selective properties of **L** were determined toward representative alkali (K⁺), alkaline earth (Ca²⁺ and Ba²⁺), and transition-metal ions (Cd²⁺, Co²⁺, Ag⁺, Ni²⁺, Cu²⁺, Zn²⁺, and Hg²⁺). Upon interaction with 100 equiv of various metal ions, only Hg²⁺ ion exhibited effective fluorescence quenching among the tested metal ions (Fig. 7a), even in the presence of other cations (e.g., Ca²⁺ and Cd²⁺, see Supplementary data).

This compound therefore possesses an efficient Hg²⁺ selective ON–OFF type signaling behavior, which can be explained by the existence of deactivation channels involving the metal orbital. The fluorescence quenching effect clearly indicates the coordination of Hg²⁺ at the receptor unit of **L**. Obviously, Hg²⁺ binds to the two nitrogen atoms, which have a lone electron pair. From the X-ray single-crystal structure of **L** (Fig. 8), the space length between the two nitrogen atoms (trialkylamine moiety) was found, which indicated that **L** could form a complex only with particular ions that have appropriate dimensions. Selected bond distances and angles are tabulated in Table 1. The dimensions of Hg²⁺ are fit to form a complex with **L**, but other metal ions do not have the suitable size. The stoichiometry of the **L**–Hg²⁺ complex was estimated to be 1:1 by ¹H NMR titration (Fig. 9) and a nonlinear curve fitting of the fluorescence titration results (Fig. 10).

As shown in the ¹H NMR spectra of Figure 9, **L** alone shows the symmetrical planar structure, which can also be seen from the single crystal (Fig. 8). Treatment with Hg²⁺ ions resulted in destroy of structural symmetry, which led to 10 signals (Fig. 9, up) from original 5 signals (Fig. 9, down) in the range of 7.2–8.2 ppm.

To gain more insight into the chemosensing properties of **L** toward Hg²⁺ ions, fluorescence titrations were carried out (Fig. 10). In high-polar solvent (5% THF+95% H₂O, Fig. 10), this system exhibited very efficient fluorescence quenching, and over 85% of the total fluorescence intensity change was observed with addition of 3 equiv of Hg²⁺ ions. The association constant, K_{assoc} , was estimated

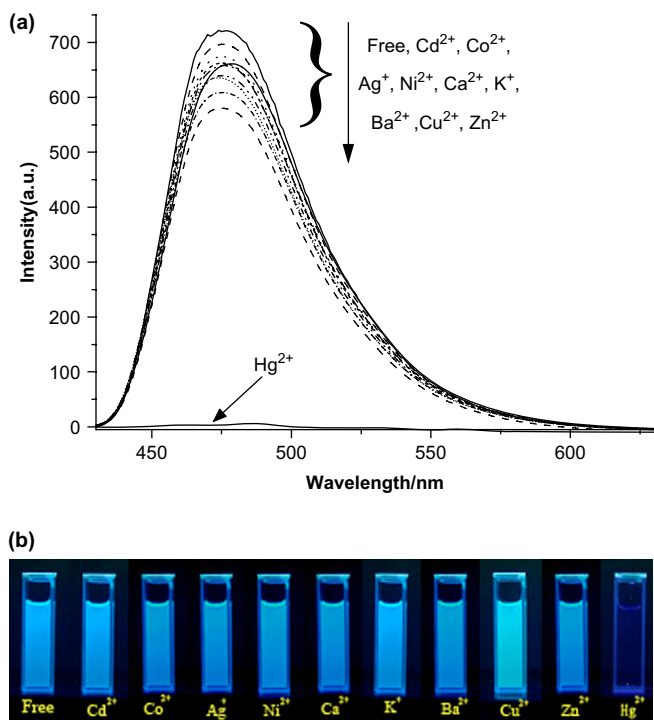


Figure 7. (a) Fluorescence spectra ($\lambda_{\text{ex}}=410$ nm) and (b) photograph (irradiated at 365 nm using UV lamp) of **L** (10 μM) with various metal ions in 50% THF solution at 298 K.

by the nonlinear curve-fitting procedure²² of fluorescence titration data and was $5.3 \times 10^4 \text{ M}^{-1}$. The detection limit²³ was also estimated from the titration results and was $2.1 \times 10^{-6} \text{ M}$.

2.4. Logic gates

Compound **L** behaves as a pH-controlled molecular switch, solvent polarity sensor, as well as Hg^{2+} sensor, which constitutes the basis for a molecular logic gate with three different logic functions (NAND, NOR, and INHIBIT) in response to solvent polarity, proton, and Hg^{2+} ion.

2.4.1. NAND gate based on a polarity–CHEQ pair

In Figure 10, we represent the quenching of fluorescence emission of **L** with Hg^{2+} in two different polarity solutions. When the solvent polarity is low (50% THF+50% H_2O , Fig. 10), relative abundant Hg^{2+} (100 equiv) was needed to quench the fluorescence

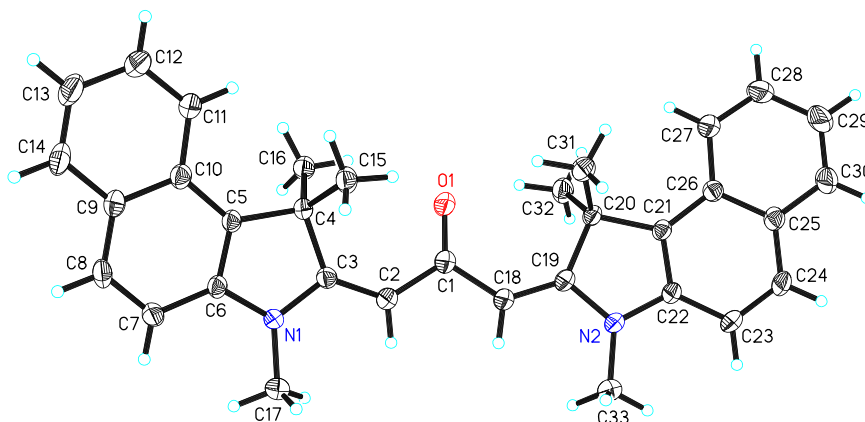


Figure 8. Perspective drawing of compound **L** with atomic numbering scheme. Thermal ellipsoids were shown at the 50% probability level.

Table 1

Selected bond distances (\AA) and bond angles ($^\circ$) for **L** with estimated standard deviations in parentheses

N(1)–C(3)	1.377(2)	C(1)–C(18)	1.459(2)
N(1)–C(17)	1.445(2)	C(1)–C(2)	1.459(2)
N(2)–C(19)	1.3769(19)	C(2)–C(3)	1.355(2)
N(2)–C(33)	1.440(2)	C(18)–C(19)	1.360(2)
C(3)–N(1)–C(17)	124.44(14)	C(2)–C(3)–N(1)	122.59(16)
C(19)–N(2)–C(33)	125.13(15)	C(19)–C(18)–C(1)	129.41(17)
C(18)–C(1)–C(2)	113.94(16)	C(18)–C(19)–N(2)	121.41(16)
C(3)–C(2)–C(1)	128.75(17)		

of **L** completely. On the other hand, when the solvent polarity is high (5% THF+95% H_2O , Fig. 10), only 3 equiv of Hg^{2+} could quench the fluorescence intensity of **L**.

Several previous reports have designed switching systems based on external inputs.¹⁸ The emission performances of chemosensors are used as the example for mimicking the logic gates. Due to the dependence of the fluorescence intensity of **L** on the external stimulations, visible light (410 nm for excitation), metal ion (Hg^{2+}), and polarity of solvent (THF/ H_2O), it is possible to mimic the function of an integrated two-input NAND logic gate (Fig. 11).

In the present system, excitation at 410 nm is the power supply. We consider the polarity of the solvent as one input—the high polarity (5% THF+95% H_2O) standing for 1 and the low one (50% THF+50% H_2O) standing for 0. The other input is the addition of 3 equiv of Hg^{2+} ions (symbol 1) or nonaddition (symbol 0). The fluorescence emission intensity ($\lambda=520$ nm) was used as the output signal as follows: if the emission reaches more than 70% of the maximum emission intensity of the free ligand in low-polarity solvent (50% THF+50% H_2O) at 520 nm, the output is considered as digital 1; if the emission lies below 10% of the maximum emission intensity, the output is considered as digital 0. The symbol of two-input NAND logic gate and the truth table is given in Figure 11.

2.4.2. NOR and INHIBIT dual-output gates based on polarity–protonation pair

Compound **L** presents a red shift of fluorescence in different polarity solvents. Meanwhile, the protonation of **L** could quench the fluorescence emission. Based on these results, compound **L** could be applied as dual-output logic gate with NOR (Out_1) and INHIBIT (Out_2) functions.

The two input signals are Input1 (high- or low-polarity solvent) and Input2 (H^+), and the two output signals are the fluorescence emissions: Output1 ($\lambda=470$ nm) and Output2 ($\lambda=520$ nm). We consider final outputs with digital 1 when the intensity of the fluorescence emission goes over 0.8 relative units, and with digital 0 when the relative intensity of the emission is below 0.3 (see Fig. 12).

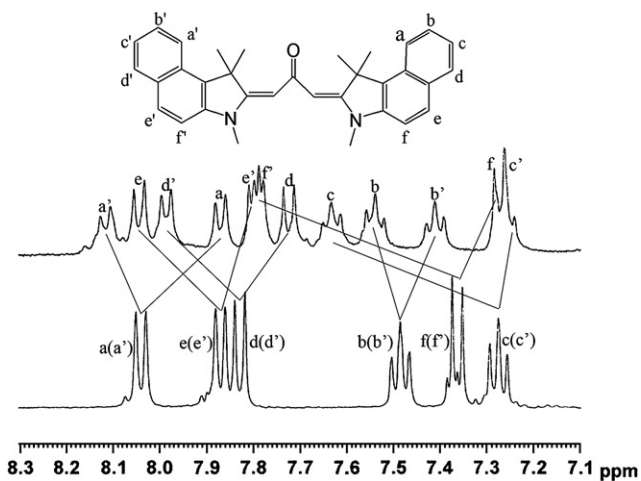


Figure 9. ^1H NMR spectra of **L** blank (down) and in the presence of Hg^{2+} ions (up) in $\text{DMSO}-d_6$. All spectra were obtained at 298 K.

When low-polarity (95% THF+5% H_2O) solvent is used (standing for 0) and at pH=8 (without H^+ , standing for 0), **L** shows only short-wavelength emission at $\lambda=470$ nm. Hence, two outputs monitoring at 470 (Out_1) and 520 nm (Out_2) result in 1 and 0, respectively.

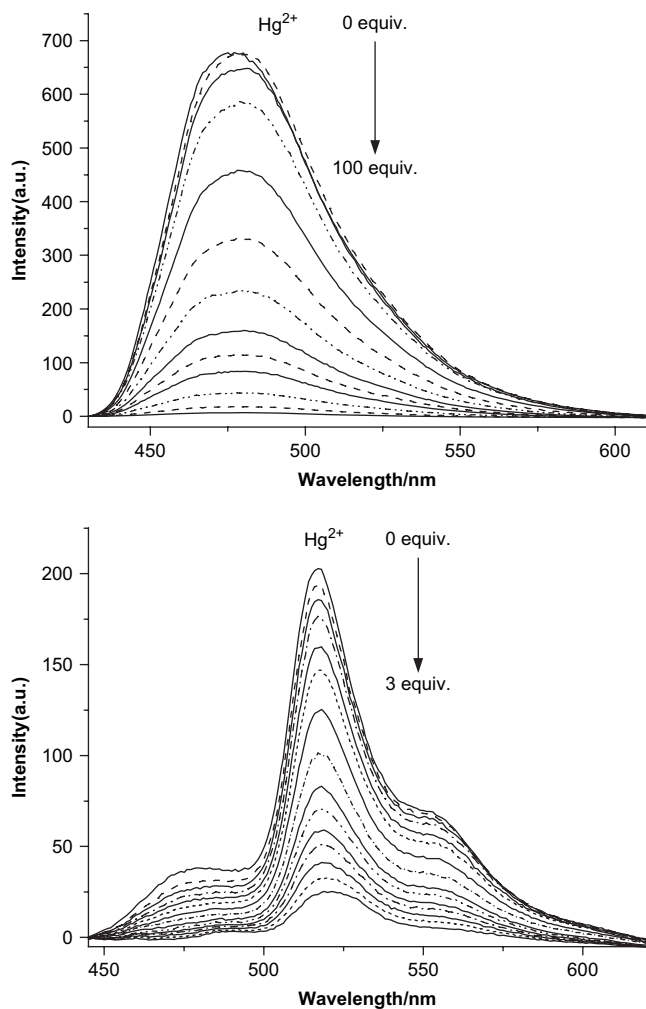


Figure 10. Change in fluorescence spectra ($\lambda_{\text{ex}}=410$ nm) of **L** (10 μM) with Hg^{2+} in low-polarity solvent (50% THF+50% H_2O , up) and high-polarity solvent (5% THF+95% H_2O , down) at 298 K.

Addition of H^+ to the solution (pH=2, Input2 is 1) leads to the protonation of **L**, which brings on quenching of fluorescence emission, resulting in 0 (Out_1) and 0 (Out_2) outputs. On the other hand, when high-polar (5% THF+95% H_2O) solvent is employed (polarity Input is 1), **L** shows long-wavelength emission at 520 nm ($\text{Output}_2=1$). Based on this diversification, a binary logic gate comes into being as shown in Figure 12.

We demonstrate that a simple-structured molecule, **L**, functions as a fluorescent molecular logic gate with multiple outputs. The most interesting feature of the present system is the fact that it can operate with solvent polarity, and, therefore, this opens new possibilities in the design of molecular logic devices. Solvent polarity, as one input, could be reset by adjusting reappportionment of different polar solvents or evaporating and re-dissolving with another polar solvent. Adding acid (e.g., HClO_4) and base (e.g., NaOH) could achieve the reversibility of protonation. Due to the fact that EDTA has stronger complexation ability with Hg^{2+} , it could be used for de-complexation of **L**- Hg^{2+} complex. However, after several operations, this system will be saturated with acid and base, as well as Hg^{2+} and EDTA. It is the ubiquitous problem for most chemical computers, which should be resolved with our efforts in the future.

3. Conclusion

A new simple and easily made merocyanine dye **L** described here displays multiple-mode fluorescence response driven by pH, solvent polarity, and Hg^{2+} ions. Controlling the multiple-mode fluorescence by simple chemical inputs resulted in three different logic functions (NAND, NOR, and INHIBIT). The potential use of this simple molecule as an efficient luminescent chemosensor as well as a molecular logic system was demonstrated.

4. Experimental section

4.1. General

The pH values were measured by using PHS-3C pH meter. ^1H NMR and ^{13}C NMR spectra were obtained by using a Bruker AV 400 spectrometer. Mass spectra were performed with an HP5989 mass spectrometer and UV-vis spectra on a Varian Cary 500 spectrophotometer (1-cm quartz cell used). Fluorescent spectra were recorded on a Varian Cary Eclipse fluorescence spectrophotometer. Toluene was distilled from calcium hydride.

4.1.1. 1,1,2,3-Tetramethyl-1H-benzo[e]indolinium iodide (**1**)¹⁷

A mixture of 60 g (0.287 mol) 1,1,2-trimethyl-1H-indole and 84 g (0.6 mol) methyl iodide was refluxed in 200 ml acetonitrile for 2 h. Upon cooling to room temperature, compound **1** was precipitated and filtered off and washed with cold diethyl ether, giving white powder. Yield: 91 g; 91%; mp 219–220 °C.

4.1.2. 2-Methylene-1,1,3-trimethyl-1H-benzo[e]indoline (**2**)¹⁷

A mixture of 20 g (0.057 mol) **1** and 7 g (0.125 mol) potassium hydroxide was stirred vigorously at room temperature in 40 ml water and 100 ml toluene for 2 h. Upon standing, the organic phase was isolated, dried (MgSO_4), and then concentrated under reduced pressure. The product was then recrystallized from ethanol to give **2** as olive flakes. Yield: 10 g; 79%; mp 107–108 °C; ^1H NMR (400 MHz, CDCl_3 , 25 °C, TMS): δ (ppm) 1.69 (s, 6H, CH_3), 3.15 (s, 3H, N- CH_3), 3.95 (d, 2H, CH_2 , $J=26.4$ Hz), 7.01 (d, 1H, $J=4.8$ Hz), 7.21 (s, 1H), 7.41 (s, 1H), 7.72 (d, 1H, $J=5.2$ Hz), 7.78 (d, 1H, $J=4.8$ Hz), 7.98 (d, 1H, $J=5.6$ Hz).

4.1.3. 1,3-Bis(1,1,3-trimethyl-1H-benzo[e]indol-2(3H)-ylidene)propan-2-one (**L**)

Compound **2** (5 g, 0.0224 mol) was stirred in 60 ml dry toluene and the temperature was kept below 5 °C. Dry pyridine (15 ml) was

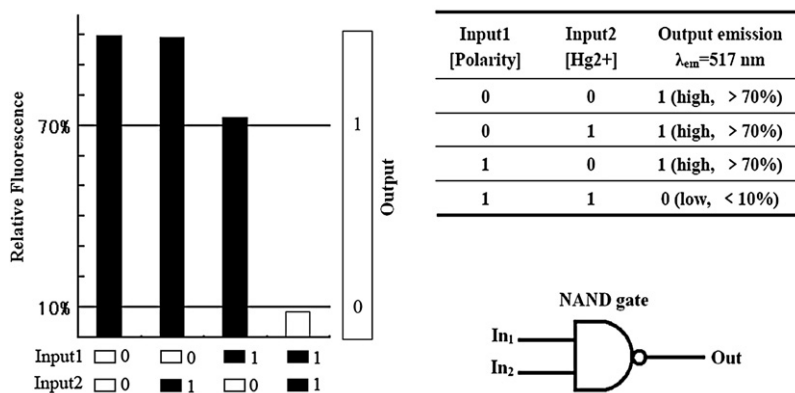


Figure 11. Bar graph representation of the output (relative fluorescence at 520 nm) of the NAND gate (excited at 410 nm at 298 K), truth table, and logic scheme.

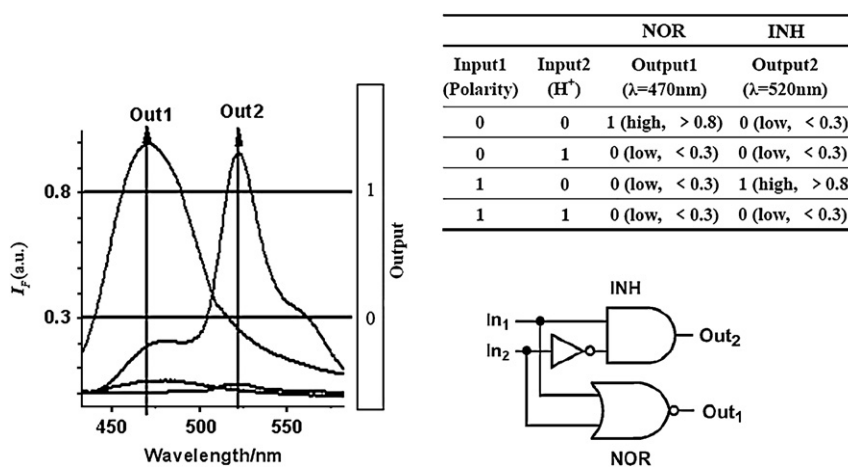


Figure 12. Fluorescence spectra ($\lambda_{ex}=410\text{ nm}$) of **L** (0.1 M) in the absence and presence of H⁺ in KCl (0.1 M) solution at 298 K, truth table, and logic scheme.

added to the mixture under stirring and isolated from water vapor. A solution of 1.11 g triphosgene (0.0112 mol) dissolved in 15 ml dry toluene was subsequently added dropwise at 0–5 °C. After the

Table 2
Crystal data and structural refinement data for **L**

Empirical formula	C ₃₃ H ₃₂ N ₂ O
Formula weight	472.61
Temperature	293(2) K
Wavelength	0.71073 Å
Crystal system	Monoclinic
Space group	P2(1)/n
Unit cell dimensions	$a=10.4999(10)\text{ Å}$, $\alpha=90^\circ$ $b=7.4272(7)\text{ Å}$, $\beta=91.258(2)^\circ$ $c=32.916(3)\text{ Å}$, $\gamma=90^\circ$
Volume	2566.3(4) Å ³
Z	4
Calculated density	1.223 g cm ⁻³
Absorption coefficient	0.073 mm ⁻¹
F(000)	1008
Crystal size	0.481 mm × 0.412 mm × 0.387 mm
θ Range for data collection	2.02–27.00°
Limiting indices	$-13 \leq h \leq 13$, $-5 \leq k \leq 9$, $-40 \leq l \leq 41$
Reflections collected/unique	14,507/5593 [$R(\text{int})=0.0809$]
Completeness to $\theta=27.00^\circ$	99.4%
Absorption correction	Empirical
Max and min transmission	1.0000 and 0.7535
Refinement method	Full-matrix least-squares on F^2
Data/restraints/parameters	5593/0/331
Goodness-of-fit on F^2	0.922
Final R indices [$I > 2\sigma(I)$]	$R1=0.0535$, $wR2=0.1232$
R indices (all data)	$R1=0.0818$, $wR2=0.1350$
Largest diff. peak and hole	0.222 and -0.222 e Å^{-3}

dropwise addition, the mixture was stirred at room temperature for 2 h and then heated at 50 °C for 5 h. Then at 0–5 °C, 2.5 g anhydrous aluminum chloride (0.0187 mol) was added and heated at 50 °C for 3 h. After cooling to room temperature, 150 ml NaOH (0.1 mol l⁻¹) was added and stirred for 10 min. Upon standing, the organic phase was isolated, washed with water (3 × 100 ml), dried (MgSO₄), and then concentrated under reduced pressure to 10 ml solution. After cooling, yellow solid (0.6 g) was precipitated and filtered off. The product was washed with ethyl acetate (20 ml) and then recrystallized from dichlorobenzene to give pure **L** as brilliant flakes. Yield: 0.52 g; 10%; mp 253–254 °C; IR (KBr, cm⁻¹): 3044, 2968, 2929, 1625, 1593, 1546, 1514, 1047, 943; ¹H NMR (400 MHz, DMSO-*d*₆, 25 °C, TMS): δ (ppm) 2.05 (s, 12H, CH₃), 3.28 (s, 6H, N-CH₃), 5.61 (t, 2H, CHCO), 7.27 (t, 2H, Ar-H), 7.36 (d, 2H, $J=8.8\text{ Hz}$, Ar-H), 7.48 (t, 2H, Ar-H), 7.85 (m, 4H, Ar-H), 8.04 (d, 2H, $J=8.8\text{ Hz}$, Ar-H); ¹³C NMR (400 MHz, DMSO-*d*₆, 25 °C, TMS): δ (ppm) 22.95 (4C, CH₃), 30.02 (2C, N-CH₃), 49.13 (2C, C(Me)₂), 99.86 (2C), 110.41 (2C), 122.31 (2C), 122.79 (2C), 127.16 (2C), 127.33 (2C), 128.71 (2C), 129.46 (2C), 129.66 (2C), 130.05 (2C), 130.18 (2C), 141.76 (1C, CO), 169.18 (2C); HRMS (ESI), m/z : 473.2577 [**L**+H]⁺.

4.2. Crystal structural determination

Single crystals of **L** were obtained by slow evaporation of dichloromethane/ethanol solution. A yellow glassy crystal of dimensions 0.481 mm × 0.412 mm × 0.387 mm was used for data collection at 20 °C ($\lambda=0.71073\text{ Å}$). Crystal data (CCDC 662222) and structural refinement data are given in Table 2. These data can be

obtained free of charge from the Cambridge Crystallographic Data Centre via www.ccdc.cam.ac.uk/data_request/cif.

Acknowledgements

This work was supported by NSFC/China (50673025, 90401026), National Basic Research 973 Program (2006CB806200), and Scientific Committee of Shanghai.

Supplementary data

Supplementary data associated with this article can be found in the online version, at doi:10.1016/j.tet.2008.05.048.

References and notes

- (a) Collier, C. P.; Wong, E. W.; Belohradsky, M.; Raymo, F. M.; Stoddart, J. F.; Kuekes, P. J.; Williams, R. S.; Heath, J. R. *Science* **1999**, *285*, 391–394; (b) Balzani, V.; Creedi, A.; Raymo, F. M.; Stoddart, J. F. *Angew. Chem., Int. Ed.* **2000**, *39*, 3348–3391; (c) Feringa, B. L. *Molecular Switches*; Wiley-VCH: Weinheim, Germany, 2001; (d) Balzani, V. *Molecular Devices and Machines: A Journey into the Nano World*; Wiley-VCH: Weinheim, Germany, 2003; (e) Margulies, D.; Melman, G.; Shanzer, A. *Nat. Mater.* **2005**, *4*, 768–771; (f) Tian, H.; Wang, Q. *Chem. Soc. Rev.* **2006**, *35*, 361–374.
- (a) Feringa, B. L.; Van Delden, R. A.; Koumura, N.; Geertsema, E. M. *Chem. Rev.* **2000**, *100*, 1789–1816; (b) Rudzinski, C. M.; Nocera, D. G. *Optical Sensors and Switches (Molecular and Supramolecular Photochemistry)*; Schanze, K. S., Ed.; Marcel Dekker: New York, NY, 2001; Chapter 1, pp 1–91; (c) Trieflinger, C.; Röhr, H.; Rurack, K.; Daub, J. *Angew. Chem., Int. Ed.* **2005**, *44*, 6943–6947; (d) Jiang, G.; Wang, S.; Yuan, W.; Jiang, L.; Song, Y. L.; Tian, H.; Zhu, D. B. *Chem. Mater.* **2006**, *18*, 235–237; (e) Amendola, V.; Fabbrizzi, L.; Foti, F.; Licchelli, M.; Mangano, C.; Pallavicini, P.; Poggi, A.; Sacchi, D.; Taglietti, A. *Coord. Chem. Rev.* **2006**, *250*, 273–299; (f) Raymo, F. M.; Tomasulo, M. *Chem.—Eur. J.* **2006**, *12*, 3186–3193; (g) Röhr, H.; Trieflinger, C.; Rurack, K.; Daub, J. *Chem.—Eur. J.* **2006**, *12*, 689–700.
- (a) Beer, P. D. *Chem. Commun.* **1996**, 689–696; (b) Atwood, J. L.; Holman, K. T.; Steed, J. W. *Chem. Commun.* **1996**, 1401–1407; (c) de Silva, A. P.; Gunaratne, H. Q. N.; Gunnaugsson, T.; Huxley, A. J. M.; McCoy, C. P.; Rademacher, J. T.; Rice, T. E. *Chem. Rev.* **1997**, *97*, 1515–1566; (d) Gale, P. A. *Coord. Chem. Rev.* **2000**, *199*, 181–233; (e) Suktai, C.; Tuntulani, T. *Chem. Soc. Rev.* **2003**, *32*, 192–202.
- (a) Fabbrizzi, L.; Licchelli, M.; Pallavicini, P. *Acc. Chem. Res.* **1999**, *32*, 846–853; (b) Raymo, F. M. *Adv. Mater.* **2002**, *14*, 401–414; (c) Brown, G. J.; de Silva, A. P.; Pagliari, S. *Chem. Commun.* **2002**, 2461–2464; (d) de Silva, A. P.; McClenaghan, N. D. *Chem.—Eur. J.* **2004**, *10*, 574–586.
- Uchiyama, S.; Kawai, N.; de Silva, A. P.; Iwai, K. *J. Am. Chem. Soc.* **2004**, *126*, 3032–3033.
- (a) Liebsch, G.; Klimant, I.; Krause, C.; Wolfbeis, O. S. *Anal. Chem.* **2001**, *73*, 4354–4363; (b) Charier, S.; Ruel, O.; Baudin, J. B.; Alcor, D.; Allemand, J. F.; Meglio, A.; Jullien, L. *Angew. Chem., Int. Ed.* **2004**, *43*, 4785–4788; (c) Wong, K. M. C.; Tang, W. S.; Lu, X. X.; Zhu, N.; Yam, V. W. W. *Inorg. Chem.* **2005**, *44*, 1492–1498; (d) Koopmans, C.; Ritter, H. J. *Am. Chem. Soc.* **2007**, *129*, 3502–3503.
- (a) de Santis, G.; Fabbrizzi, L.; Licchelli, M.; Sardone, N.; Velders, A. H. *Chem.—Eur. J.* **1996**, *2*, 1243–1250; (b) Fabbrizzi, L.; Licchelli, M.; Mascheroni, S.; Poggi, A.; Sacchi, D.; Zema, M. *Inorg. Chem.* **2002**, *41*, 6129–6136; (c) Zhang, G.; Zhang, D.; Guo, X.; Zhu, D. *Org. Lett.* **2004**, *6*, 1209–1212; (d) Zapata, F.; Caballero, A.; Espinosa, A.; Tárraga, A.; Molina, P. *Org. Lett.* **2007**, *9*, 2385–2388.
- (a) Fichou, D.; Hubert, C.; Garnier, F. *Adv. Mater.* **1995**, *7*, 914–917; (b) Zhang, G.; Yang, G.; Wang, S.; Chen, Q.; Ma, J. S. *Chem.—Eur. J.* **2007**, *13*, 3630–3635; (c) Zhao, Z.; Xing, Y. J.; Wang, Z. X.; Lu, P. *Org. Lett.* **2007**, *9*, 547–550; (d) Silva, P. L.; Bastos, E. L.; El Seoud, O. A. *J. Phys. Chem. B* **2007**, *111*, 6173–6180.
- (a) de Silva, A. P.; Gunaratne, H. Q. N.; McCoy, C. P. *J. Am. Chem. Soc.* **1997**, *119*, 7891–7892; (b) Bodenant, B.; Fages, F.; Delville, M. M. *J. Am. Chem. Soc.* **1998**, *120*, 7511–7519; (c) de Silva, S. A.; Amorelli, B.; Isidor, D. C.; Loo, K. C.; Crooker, K. E.; Pena, Y. E. *Chem. Commun.* **2002**, 1360–1361; (d) Rurack, K.; Resch-Genger, U. *Chem. Soc. Rev.* **2002**, *31*, 116–127; (e) Yang, R. H.; Chan, W. H.; Lee, A. W. M.; Xia, P. F.; Zhang, H. K.; Li, K. J. *Am. Chem. Soc.* **2003**, *125*, 2884–2885.
- Shiraishi, Y.; Tokitoh, Y.; Hirai, T. *Chem. Commun.* **2005**, 5316–5318.
- (a) Brooker, L. G. S.; Keyes, G. H.; Sprague, R. H.; VanDyke, R. H.; VanLare, E.; Van Zandt, G.; White, F. L.; Cressman, H. W. J.; Dent, S. G. *J. Am. Chem. Soc.* **1951**, *73*, 5332–5350; (b) Tian, H.; Meng, F. S. *Functional Dyes*; Kim, S. H., Ed.; Elsevier: Amsterdam, 2006; Chapter 2, pp 47–84; (c) Marder, S. R. *Chem. Commun.* **2006**, 131–134.
- (a) Toutchkine, A.; Kraynov, V.; Hahn, K. *J. Am. Chem. Soc.* **2003**, *125*, 4132–4145; (b) Nalbant, P.; Hodgson, L.; Kraynov, V.; Toutchkine, A.; Hahn, K. M. *Science* **2004**, *305*, 1615–1619.
- (a) Lakowicz, J. R. *Principles of Fluorescence Spectroscopy*; Plenum: New York, NY, 1999; (b) Valeur, B. *Molecular Fluorescence: Principles and Applications*; Wiley-VCH: Weinheim, 2002.
- (a) Balzani, V.; Creedi, A.; Venturi, M. *ChemPhysChem.* **2003**, *4*, 49–59; (b) de Silva, A. P.; Uchiyama, S. *Nat. Nanotechnol.* **2007**, *2*, 399–410.
- (a) Weiss, S. *Science* **1999**, *283*, 1676–1683; (b) Zang, L.; Liu, R.; Holman, M. W.; Nguyen, K. T.; Adams, D. M. *J. Am. Chem. Soc.* **2002**, *124*, 10640–10641; (c) Qu, D. H.; Wang, Q. C.; Tian, H. *Angew. Chem., Int. Ed.* **2005**, *44*, 5296–5299.
- Some examples: (a) de Silva, A. P.; Gunaratne, H. Q. N.; McCoy, C. P. *Nature* **1993**, *364*, 42–44; (b) Creedi, A.; Balzani, V.; Langford, S. J.; Stoddart, J. F. *J. Am. Chem. Soc.* **1997**, *119*, 2679–2681; (c) Baytekin, H. T.; Akkaya, E. U. *Org. Lett.* **2000**, *2*, 1725–1727; (d) Stojanovic, M. N.; Mitchell, T. E.; Stefanovic, D. *J. Am. Chem. Soc.* **2002**, *124*, 3555–3561; (e) Guo, X. F.; Zhang, D. Q.; Wang, T. X.; Zhu, D. B. *Chem. Commun.* **2003**, 914–915; (f) Guo, X. F.; Zhang, D. Q.; Zhang, G. X.; Zhu, D. B. *J. Phys. Chem. B* **2004**, *108*, 11942–11945; (g) Tang, Y. L.; He, F.; Wang, S.; Li, Y. L.; Zhu, D. B.; Bazan, G. C. *Adv. Mater.* **2006**, *18*, 2105–2110; (h) Qu, D. H.; Ji, F. Y.; Wang, Q. C.; Tian, H. *Adv. Mater.* **2006**, *18*, 2035–2038.
- Wang, J.; Cao, W. F.; Su, J. H.; Tian, H.; Sun, Z. R. *Dyes and Pigments* **2003**, *57*, 171–179.
- (a) Akkaya, E. U.; Huston, M. E.; Czarnik, A. W. *J. Am. Chem. Soc.* **1990**, *112*, 3590–3593; (b) de Silva, A. P.; Fox, D. B.; Huxley, A. J. M.; Moody, T. S. *Coord. Chem. Rev.* **2000**, *205*, 41–57; (c) Amendola, V.; Fabbrizzi, L.; Mangano, C.; Miller, H.; Pallavicini, P.; Parotti, A.; Taglietti, A. *Angew. Chem., Int. Ed.* **2002**, *41*, 2553–2556; (d) Shiraishi, Y.; Tokitoh, Y.; Hirai, T. *Org. Lett.* **2006**, *8*, 3841–3444; (e) Shiraishi, Y.; Tokitoh, Y.; Nishimura, G.; Hirai, T. *J. Phys. Chem. B* **2007**, *111*, 5090–5100.
- (a) Brooker, L. G. S.; Keys, C. H.; Heseltine, D. W. *J. Am. Chem. Soc.* **1951**, *73*, 5350–5356; (b) Reichardt, C. *Solvents and Solvent Effects in Organic Chemistry*; Chemie: New York, NY, 1988; (c) Reichardt, C. *Chem. Rev.* **1994**, *94*, 2319–2358.
- Weisenborn, P. C. M.; Huizer, A. H.; Varma, C. A. G. O. *Chem. Phys.* **1988**, *126*, 425–433.
- (a) Yoon, J.; Ohler, N. E.; Vance, D. H.; Aumiller, W. D.; Czarnik, A. W. *Tetrahedron Lett.* **1997**, *38*, 3845–3848; (b) Prodi, L.; Bargossi, C.; Montalti, M.; Zaccaroni, N.; Su, N.; Bradshaw, J. S.; Izatt, R. M.; Savage, P. B. *J. Am. Chem. Soc.* **2000**, *122*, 6769–6770; (c) Moon, S. Y.; Cha, N. R.; Kim, Y. H.; Chang, S. K. *J. Org. Chem.* **2004**, *69*, 181–183; (d) Liu, B.; Tian, H. *Chem. Commun.* **2005**, 3156–3158; (e) Guo, Z. Q.; Zhu, W. H.; Shen, L. J.; Tian, H. *Angew. Chem., Int. Ed.* **2007**, *46*, 5549–5553.
- Nishizawa, S.; Cui, Y. Y.; Minagawa, M.; Morita, K.; Kato, Y.; Taniguchi, S.; Kato, R.; Teramae, N. *J. Chem. Soc., Perkin Trans. 2* **2002**, 866–870.
- Shortreed, M.; Kopelman, R.; Kuhn, M.; Hoyland, B. *Anal. Chem.* **1996**, *68*, 1414–1418.